ORGANIC CHEMISTRY FRONTIERS

CCS 中国化学会 CHINESE CHEMICAL SOCIETY

SIOC 1950

ROYAL SOCIETY OF CHEMISTRY

Carbazol-3-olate photosensitizers enable photocatalytic hydrodefluorination and Birch-type reduction reactions

Journal:	*Organic Chemistry Frontiers*
Manuscript ID	QO-RES-01-2025-000056.R1
Article Type:	Research Article
Date Submitted by the Author:	15-Mar-2025

Complete List of Authors:	Kuang, Huilong; Kobe University Xie, Weibin; Kobe University Yabuta, Tatsushi; Kobe University Fuki, Masaaki; Kobe University Higashi, Masahiro; Nagoya University, Graduate School of Informatics Kobori, Yasuhiro; Kobe University, Molecular Photoscience Research Center Sakai, Nozomi; Kobe University Akimoto, Seiji; Kobe University, Molecular Photoscience Research Center Hayashi, Masahiko; Kobe University, Chemistry, Graduate School of Science Matsubara, Ryosuke; Kobe University,

ARTICLE

Carbazol-3-olate photosensitizers enable photocatalytic hydrodefluorination and Birch-type reduction reactions

Received 00th January 20xx,
Accepted 00th January 20xx

DOI: 10.1039/x0xx00000x

Huilong Kuang,[a] Weibin Xie,*[a] Tatsushi Yabuta,[a] Masaaki Fuki,[ab] Masahiro Higashi,[c] Yasuhiro Kobori,*[ab] Nozomi Sakai,[a] Seiji Akimoto,[ab] Masahiko Hayashi,[a] Ryosuke Matsubara*[a]

Despite significant recent advances in the development of organic photosensitizers (PSs), designing a PS with both long-wavelength absorption and high reducing ability remains challenging. In this study, we introduce carbazol-3-olates as a novel class of PSs that exhibit these desirable properties. Compared to their neutral carbazole counterparts, anionic carbazol-3-olates exhibited a 70-nm red-shift in absorption and a 0.54-V negative shift in the excited-state reduction potential. The use of carbazol-3-olates as PSs enabled photocatalysis of hydrodefluorination and Birch-type reduction reactions under long-wavelength visible-light irradiation. Furthermore, the Birch reduction reactions exhibited tolerance toward aqueous environments when conducted using our PS, thus expanding their industrial applicability. Mechanistic studies revealed electron transfer from the excited carbazol-3-olates to inert substrates, such as fluoroarenes, highlighting the high catalytic efficiency of carbazol-3-olates as PSs for reduction reactions. Therefore, with their transition-metal-free nature and facile synthesis process, we expect carbazol-3-olates to be industrially advantageous PSs for catalyzing challenging photochemical reduction reactions.

Introduction

Photosensitizers (PSs), upon excitation by light, can transfer electrons to substrates, thus initiating various chemical reactions. Organic PSs have garnered significant attention in the scientific community as novel materials with promising potential for photonic energy conversion owing to their low toxicities, cost-effectiveness, and easy accessibility compared to transition-metal-containing PSs.[1] Currently, multiple studies have reported the use of PSs to facilitate reduction reactions through electron transfer (ET) processes under visible-light irradiation. However, the achievement of photochemical hydrodefluorination and Birch reduction, the substrates of which have extremely low reduction potentials, remains a formidable challenge owing to the limited reducing ability of conventional PSs (Scheme 1a). Therefore, these reactions have typically relied on highly reactive alkali metals under stringent conditions or transition-metal catalysts combined with reductants. Recent studies have reported several PSs with potent reduction capabilities that can facilitate these formidable reactions under visible light irradiation.[2] Miyake employed benzo[ghi]perylene imides as photocatalysts to achieve the Birch-type reduction of unactivated arenes, based on the concept of consecutive photoinduced electron transfer.[3] König utilized an iridium-based PS to enable Birch-type reactions of activated polycyclic arenes via the sensitized ET strategy.[4] Weaver, as well as Cheng and Tan, used transition-metal-based PSs to activate the C–F bonds of activated fluoroarenes.[5-6] Kominami, Matsubara, and Iwasawa reported the hydrodefluorination of unactivated fluoroarenes using transition-metal-based or organic PSs.[7-9] However, several issues remain to be addressed for each reported reaction, such as the use of transition metals, requirement of ultraviolet (UV) irradiation and/or activated substrates, low reaction efficiencies, and complicated synthesis methods for PSs.

Based on pioneering studies,[10-11] the field of photochemical reduction has recently witnessed the development of anionic PSs that demonstrate exceptional reducing abilities and desirable photophysical properties (Scheme 1b).[12-13] Hasegawa reported a naphtholate-based PS to catalyze reductive desulfonylation reactions.[14] Xia developed a phenolate-based PS to enable the cleavage of the C–X bonds of iodo-, bromo-, and chloroarenes.[15-16] König developed an anthrolate-based PS that was applied for the carboxylation of (hetero)arenes and styrene derivatives.[17] Melchiorre developed an indole thiolate-based PS that catalyzed both the C–X bond activation of haloarenes (X = Cl, F, $OPO(OEt)_2$) and Birch-type reduction.[18] Shang reported defluoroalkylation and hydrodefluorination of trifluoromethyls using *o*-phosphinophenolates.[19-21] Dell'Amico and Filippini developed sulfone-pendant phenols as PSs that catalyzed iodosulfonylation of olefins.[22]

Our group has focused on the development of carbazole-based PSs.[23-24] Carbazole has an electron-rich nitrogen-containing heteroaromatic skeleton, and the parent carbazole has a

[a] Department of Chemistry, Graduate School of Science, Kobe University, 1-1 Rokkodai-cho, Nada-ku, Kobe 657-8501, Japan. E-mail: weibinxie@people.kobe-u.ac.jp, ykobori@kitty.kobe-u.ac.jp, matsubara.ryosuke@people.kobe-u.ac.jp.
[b] Molecular Photoscience Research Center, Kobe University, 1–1 Rokkodai–cho, Nada–ku, Kobe 657–8501, Japan.
[c] Department of Complex Systems Science, Graduate School of Informatics, Nagoya University, Nagoya, 464-8601, Japan.

† Supplementary Information available: [details of any supplementary information available should be included here]. See DOI: 10.1039/x0xx00000x

relatively long-wavelength absorption maximum of 334 nm, which corresponds to electronic transition from the highest occupied molecular orbital (HOMO) to the lowest unoccupied molecular orbital (LUMO).[25] As the HOMO coefficients at the 3- and 6-positions of carbazole are large and those of LUMO are small, incorporating electron-donating groups at the 3- and 6-positions increases the energy level of the HOMO and has little effect on that of the LUMO, resulting in a decrease in the HOMO–LUMO gap, which leads to a red-shift of the absorption spectrum.[26] Based on this concept, we recently discovered 3,6-bis(dimethylamino)carbazole and its derivatives as potential PSs, with broad visible light absorption (λ_{max} = 400 nm) and high reducing ability (E^*_{ox} = –2.75 V vs SCE). These carbazole PSs successfully catalyzed the demanding reductive activation of C–X bonds (X = Cl, F, OR) and CO_2 reduction to formate.[8, 27-29] With this background, we were motivated to develop PSs using carbazol-3-olate, an anionic carbazole molecule with an oxyanion, a strong electron-donating substituent, at the 3-position, to achieve improved catalytic properties with relatively simple structural manipulation (Scheme 1c).[30-31]

Herein, we report the synthesis and optoelectronic properties of carbazol-3-olate PSs and their successful catalysis of hydrodefluorination and Birch-type reduction reactions. We tested various PSs and investigated the reaction conditions for the two reactions, and successfully showed that our carbazole-3-olate PSs could facilitate the reactions under long-wavelength visible light irradiation without the need for transition metals. We also investigated the substrate scopes and proposed mechanisms for the two reactions.

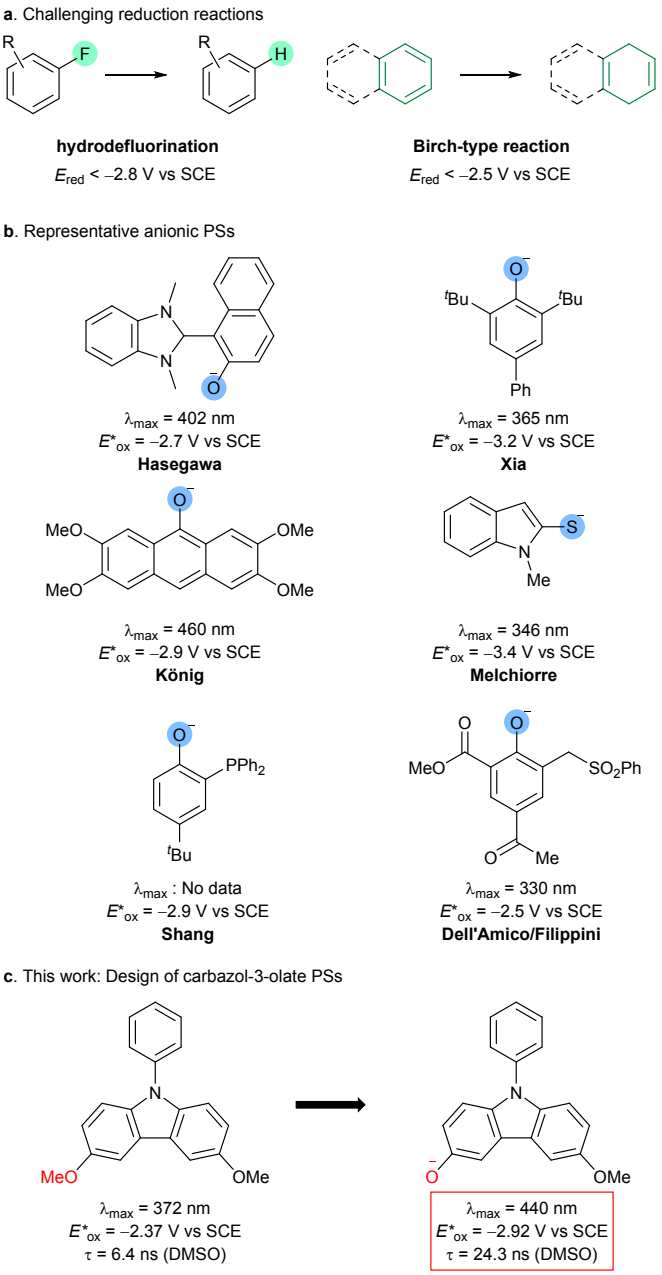

Scheme 1 (a) Challenging reduction reactions. (b) Reported representative anionic photosensitizers (PSs). [14-19, 22] (c) This work: development of carbazol-3-olate PSs for photocatalyzing formidable reduction reactions.

Results and Discussion

Based on the assumption that the in situ deprotonation of carbazol-3-ol in the presence of a base leads to the formation of carbazol-3-olate owing to the acidity of phenolic protons, several carbazol-3-ol derivatives were synthesized for the study and directly utilized in photochemical reactions under basic conditions. Of these, the carbazol-3-ols **PS1** and **PS4** and carbazol-3,6-diols **PS3** and **PS5** were selected as the research targets (Fig. 1a). They can all be synthesized by the facile demethylation of the corresponding methoxycarbazole derivatives using pyridine hydrochloride (see Supporting Information Section S3 for the details). Furthermore, **PS2** and

PS6, which do not have anionic natures, were also employed as controls.[24, 28]

The hydrodefluorination of 4-fluoroanisole (E_{red} = <–3.0 V vs SCE) in DMSO[32] was investigated using 2 mol% of the PS, 3 equiv of Cs_2CO_3, and 4 equiv of potassium formate under 440-nm visible light irradiation (Fig. 1b, see Table S2 for the complete list of experiments). **PS1** afforded the desired reduced product anisole in 95% yield after 24 h. Control experiments revealed that light, Cs_2CO_3, and the PS were all indispensable for the reaction progress (Fig. 1b, entry 1). Furthermore, the reaction proceeded in low yield in the absence of potassium formate (12% yield; Fig. 1b, entry 2). The electron source in this case is unknown. To our delight, the reaction still proceeded under visible light irradiation when the λ_{max} = 480 nm (Fig. 1b, entry 3), suggesting that **PS1** has a potential for future applications involving long-wavelength light. Meanwhile, **PS2**, which had no acidic protons, showed poor reactivity (Fig. 1b, entry 4), probably owing to a lack of visible-light absorption (vide infra). The use of the carbazol-3,6-diol **PS3** also provided the product, albeit in slightly lower yield than achieved using **PS2** (Fig. 1b, entry 5). When the reaction time was reduced to 6 h instead of 24 h, the product yields were 43% and 66% when using **PS1** and **PS3**, respectively, indicating that **PS3** exhibited higher catalytic activity but lower durability under the irradiation conditions than **PS1**. The use of the 9-non-substituted carbazole variants **PS4** and **PS5** and the dimethylamino group-substituted carbazole **PS6** (E^*_{ox} = –2.7 V vs SCE)[28] afforded inferior results to those achieved using **PS1** (Fig. 1b, entries 6–8).[33] The reaction should theoretically proceed with a catalytic amount of Cs_2CO_3; however, using less than 3 equivalents resulted in a lower yield. This can be attributed to the equilibrium-driven promotion of **PS1** deprotonation with higher Cs_2CO_3 loading and the contribution of Cs cation to substrate activation.[33]

Next, the optoelectronic properties of the carbazol-3-olates were investigated. Absorption spectroscopy revealed that **PS1** absorbed only UV-region light in the absence of a base (Fig. 1c). Unsurprisingly, the absorption spectrum of **PS2** was almost identical to that of **PS1**, as the electronic states of the carbazole chromophore cores of **PS1** and **PS2** were similar. Therefore, in subsequent experiments, **PS2** was used as a substitute for non-deprotonated **PS1** when comparing with deprotonated **PS1**, because **PS2** was not affected by the inadvertent hydrogen bonding that might have occurred in the case of **PS1**. In the presence of Cs_2CO_3, **PS1** exhibited visible light absorption with a long-wavelength absorption maximum of 440 nm, indicating that the deprotonation of the hydroxy group formed a carbazol-3-olate structure that was electronically distinct from the carbazol-3-ol structure. The ^{1}H nuclear magnetic resonance (NMR) spectroscopic analysis of the solution of **PS1** in the presence of Cs_2CO_3 also suggested the deprotonation of the hydroxyl group (Fig. S2). The red shift in absorption resulting from the deprotonation can be explained by an increase in the HOMO energy level caused by the interaction between the HOMO and the electron-donating oxide substituent, leading to a decrease in the HOMO–LUMO gap (Fig. S9). The results of time-dependent density-functional theory calculations well-matched the experimental absorption spectra (Fig. S10). Furthermore, carbazol-3-olate species derived from **PS1** were emissive (Fig. 1d), indicating that the excited state of the anionic carbazol-3-olate could relax to the ground state via a radiative pathway. Note that the carbazol-3,6-diol **PS3**, when in the presence of Cs_2CO_3, exhibited absorption and fluorescence spectra similar to those of deprotonated **PS1** (Fig.s S4 and S5), which indicates that only one hydroxy group of the two in **PS3** was deprotonated by Cs_2CO_3 (see Supporting Information Section S4 for details). The absorption and emission spectra of **PS4** and **PS5** in the presence and absence of Cs_2CO_3 are shown in the Supporting Information (Fig.s S6–S8).

The oxidation potential of deprotonated **PS1** shifted by approximately 1 V in the negative direction upon deprotonation (Fig. 1e), indicating that it became more electron-rich and, thus, more susceptible to oxidation compared to its state prior to deprotonation. The oxidation potentials of **PS2** and deprotonated **PS3**, **PS4**, and **PS5** are shown in the Supporting Information (Fig. S12).

The measured fluorescence quantum yields and fluorescence lifetimes as well as the aforementioned optoelectronic data are shown in Fig. 1f. The oxidation potential of deprotonated **PS1** at its excited state (E_{ox}* = –2.92 V vs SCE), which was calculated from its ground state oxidation potential and excitation energy,[1] was notably lower by 0.54 V than that of **PS2** (E_{ox}* = –2.38 V vs SCE), demonstrating that the deprotonation of the hydroxy group of the PS significantly enhanced its electron-donating ability (Section S6). Furthermore, the fluorescence lifetime of deprotonated **PS1** was 4 times longer (τ = 24.3 ns) than that of non-deprotonated **PS2** (τ = 6.4 ns) (Section S7). Both the radiative (k_r) and non-radiative (k_{nr}) decay rates were lower for deprotonated **PS1**, with the radiative decay rate, in particular, decreasing by an order of magnitude. The k_r values calculated with the harmonic approximation were 1.4×10^7 s^{-1} for deprotonated **PS1** and 5.7×10^7 s^{-1} for **PS2**, which are in reasonable agreement with the experimental values (0.5×10^7 s^{-1} for deprotonated **PS1** and 5.5×10^7 s^{-1} for **PS2**). The difference in calculated rates mainly originated from the difference in fluorescence energy. The overestimation of the k_r of deprotonated **PS1** could be due to the anharmonicity from the strong interaction between the **PS1** anion and DMSO solvent (see Section S5 for details). The small k_{nr} (3.6×10^7 s^{-1}) for deprotonated **PS1** also contributed to the elongation of the fluorescence lifetime. Considering the k_{nr} as dominated by the intersystem crossing (ISC) in carbazole, this suggests that the ISC rate from the S_1 of deprotonated **PS1** decreased because of a significant reduction in the S_1–T_1 energy gap, hindering the spin-orbit coupling between the S_1 and T_n states prior to the T_n–T_1 internal conversion.

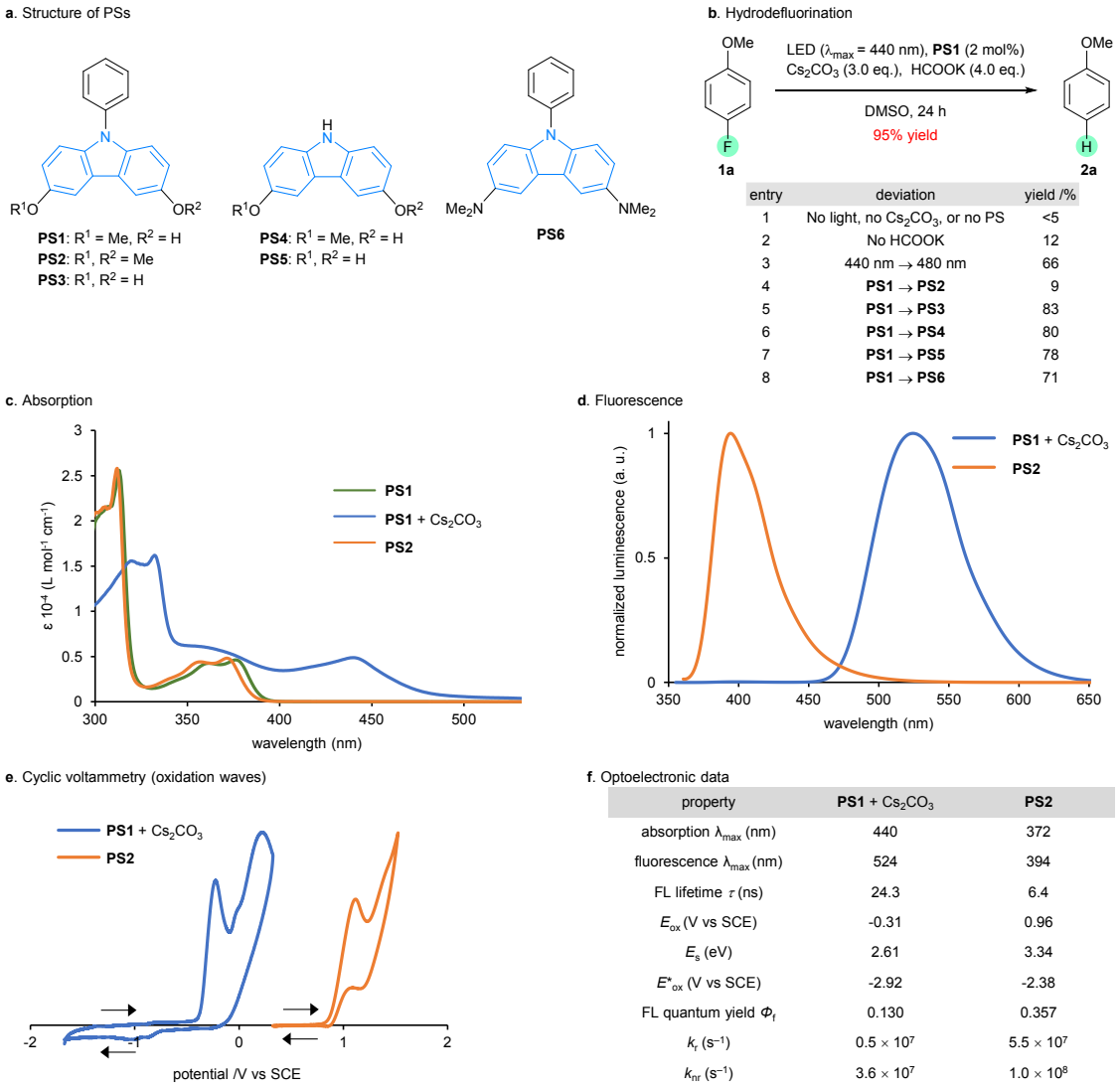

entry	deviation	yield /%
1	No light, no Cs_2CO_3, or no PS	<5
2	No HCOOK	12
3	440 nm → 480 nm	66
4	**PS1** → **PS2**	9
5	**PS1** → **PS3**	83
6	**PS1** → **PS4**	80
7	**PS1** → **PS5**	78
8	**PS1** → **PS6**	71

f. Optoelectronic data

property	**PS1** + Cs_2CO_3	**PS2**
absorption λ_{max} (nm)	440	372
fluorescence λ_{max} (nm)	524	394
FL lifetime τ (ns)	24.3	6.4
E_{ox} (V vs SCE)	-0.31	0.96
E_s (eV)	2.61	3.34
E^*_{ox} (V vs SCE)	-2.92	-2.38
FL quantum yield Φ_f	0.130	0.357
k_r (s^{-1})	0.5×10^7	5.5×10^7
k_{nr} (s^{-1})	3.6×10^7	1.0×10^8

Fig. 1 (a) Structures of the employed carbazole-based PSs. (b) Hydrodefluorination using the carbazol-3-olate PSs. (c) Absorption spectra of **PS1**, **PS1** with Cs_2CO_3, and **PS2** in DMSO. (d) Florescence spectra of **PS1** with Cs_2CO_3 and **PS2** in DMSO. Excitation wavelength: 350 nm. (e) Cyclic voltammograms (oxidation waves) of **PS1** with Cs_2CO_3 and **PS2** in DMSO. (f) Summary of optoelectronic data of **PS1** with Cs_2CO_3 and **PS2**. E_{ox}: Oxidation potentials of ground-state molecules obtained from cyclic voltammetry analysis (Fig. 1e). E_S: Singlet excited state energies approximated from the fluorescence spectra (Fig. 1d). E_{ox}^*: Oxidation potential of the singlet excited states of the molecules, as calculated using the equation $E_{ox}^* = E_{ox} - E_s$. k_r: Radiative decay rate constant calculated using $k_r = \Phi/\tau$. k_{nr}: Nonradiative decay rate constant calculated using $k_{nr} = (1-\Phi)/\tau$. See also: Table S1 in the Supporting Information.

Next, we investigated the scope of substrates for hydrodefluorination (Fig. 2). Electronically neutral or electron-donating group-substituted aryl fluorides **1b–f** provided the hydrodefluorinated products in high yields upon using 2 mol% of **PS1**. The reaction with substrate **1g** proceeded sluggishly even with 5 mol% of **PS1**, affording the product in moderate yield along with unidentified byproducts. The substrate **1h**, which had two methyl groups at the ortho positions to a fluorine atom, achieved an excellent yield of 90% upon using 5 mol% of **PS1**. The aryl fluorides **1i** and **1j** that possess electron-withdrawing groups, as well as the electron-deficient aromatics **1k** and **1l**, afforded the products in moderate yields. In general, the photochemical hydrodefluorination of electron-deficient substrates proceeds more slowly than that of electron-rich ones, likely due to the slow C–F bond cleavage following the electron transfer event.[9] Benzotrifluoride was used as a substrate under the established reaction conditions; however, compounds in which one or more fluorine atoms were simply replaced by hydrogen were scarcely obtained.

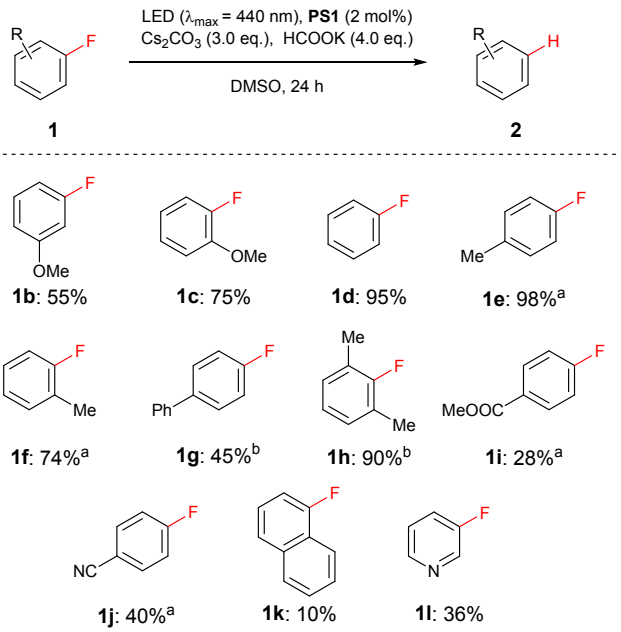

Fig. 2 Substrate scope for the hydrodefluorination reaction. Conditions: LED irradiation (λ_{max} = 440 nm), **PS1** (2 mol%), HCOOK (4.0 equiv), Cs_2CO_3 (3.0 equiv), aryl fluoride **1** (1.0 equiv) in DMSO (0.1 M), argon atmosphere, 24 h. The NMR yields are shown. [a] GC yield. [b] 5 mol% **PS1**.

We then investigated the application of the carbazol-3-olate PSs for photochemical Birch-type reduction reactions. Recently, elegant photochemical Birch-type reduction reactions have been developed; however, they require either short-wavelength light or transition metal-based photocatalysts.[4, 18] We expected that the developed transition metal-free carbazol-3-olate PSs could catalyze Birch-type reduction reactions with longer wavelength light. In our study, the Birch-type reduction of naphthalene (**3a**) successfully proceeded upon using **PS1** under 440-nm irradiation in the presence of 1 equiv of Cs_2CO_3 and 6 equiv of iPr$_2$NEt, affording 1,4-dihydronaphthalene (**4a**) in 74% yield (Table 1, entry 1). The reaction also proceeded under visible light irradiation with λ_{max} = 480 nm, with only a marginal decrease in yield (Table 1, entry 2). Control experiments demonstrated that light, iPr$_2$NEt, PS, and Cs_2CO_3 were essential for Birch-type reduction (Table 1, entries 3–5). Replacing iPr$_2$NEt with potassium formate, the choice of electron donor for the hydrodefluorination reaction, decreased the product yield (Table 1, entry 6). Notably, adding up to 10 equiv of water did not alter the product yield (Table 1, entry 7), suggesting that this catalytic system using **PS1** exhibits tolerance toward aqueous environments, which is in sharp contrast to the standard Birch reactions conducted using zero-valent alkali metals. Among the tested PSs, **PS1** provided the highest product yield (Table 1, entry 1 vs entries 8–12).

We then investigated the substrate scope for the developed Birch-type reduction reaction (Fig. 3). The mono-substituted naphthalene derivatives **3b–3g** were subjected to the established reaction conditions: the 1-substituted naphthalene derivatives (**3b**, **3d**, **3f**, and **3g**) afforded di-hydro products with aromaticity remaining on the ring side with a substituent, while, in contrast, the 2-substituted naphthalene derivatives (**3c** and **3e**) afforded a mixture of products favoring di-hydro products, with the aromaticity remaining on the non-substituted ring side. When 1-fluoronaphthalene (**3g**) was used as a substrate, the formation of product **4a** was also observed, likely generated through hydrodefluorination either before or after the Birch-type reduction process. The reduction of phenanthrene (**3h**) resulted in hydrogenation at the 9- and 10-positions, affording the biphenyl derivative **4h** in 74% yield. The heteroaromatics benzofuran (**3i**) and benzo[b]thiophene (**3j**) also underwent Birch-type reduction, leading to the formation of **4i** and **4j**, respectively; the products were dehydrogenated at the 2- and 3-positions. A list of low-reactive substrates is provided in Fig. S15.

Table 1 Reaction conditions and yields for the Birch-type reduction of naphthalene

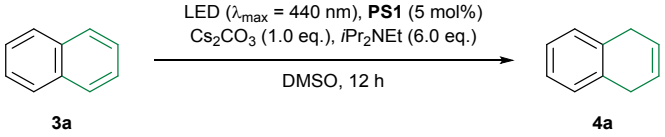

Entry	Deviation from Reaction Conditions	Yield /%[a]
1	None	74
2	440 nm → 480 nm	62
3	No light or no iPr$_2$NEt	0
4	No PS	11
5	No Cs_2CO_3	8
6	iPr$_2$NEt → HCOOK	39
7	H_2O (10 eq.) added	74
8	**PS1** → **PS2**	34
9	**PS1** → **PS3**	< 5
10	**PS1** → **PS4**	< 5
11	**PS1** → **PS5**	9
12	**PS1** → **PS6**	54

[a] NMR yield.

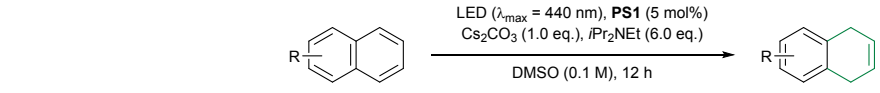

substrate	product	substrate	product
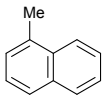 **3b**	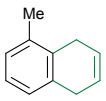 **4b** : 63%	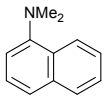 **3f**	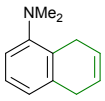 **4f**: 58%
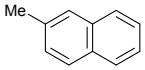 **3c**	 **4c** : 56% **4c'** : 28%	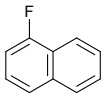 **3g**	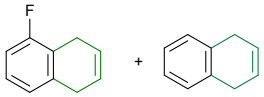 **4g:** 35% **4a:** 32%
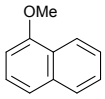 **3d**	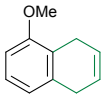 **4d** : 69%	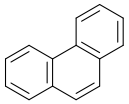 **3h**	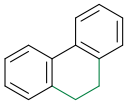 **4h:** 74%
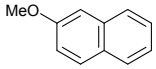 **3e**	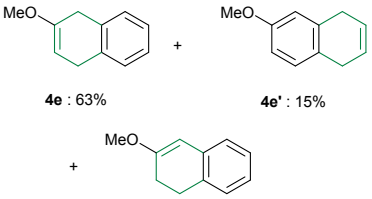 **4e** : 63% **4e'** : 15% **4e''** : 12%	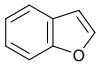 **3i**	 **4i:** 45%[a]
		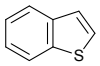 **3j**	 **4j**: 27%

[a] 24 h.

Fig. 3 Substrate scope for Birch-type reduction. The NMR yields are shown.

To elucidate the mechanisms underlying the hydrodefluorination and Birch-type reduction reactions, we performed fluorescence-quenching experiments on deprotonated **PS1**, utilizing 4-fluoroanisole **1a** and naphthalene **3a** as the quenchers. In both cases, the fluorescence of the excited deprotonated **PS1** was quenched; the quenching rate constants (k_q) obtained upon using **1a** and **3a** were 3.4×10^7 and 5.9×10^9 L mol^{-1} s^{-1}, respectively (Fig. 4 and Section S9). The possibility of the formation of an electron donor–acceptor complex or an exciplex between the deprotonated **PS1** and either substrate **1a** or **3a** was ruled out (Sections S10 and S11). The proposed reaction mechanism for hydrodefluorination is delineated in Fig. 5a. In this reaction, the carbazole **PS1** loses a proton from its hydroxy group in the presence of Cs_2CO_3, resulting in the formation of carbazol-3-olate **5**, an active PS. Upon excitation with visible light, the excited carbazol-3-olate **5*** (E^*_{ox} = –2.92 V vs SCE) is generated, which undergoes ET with

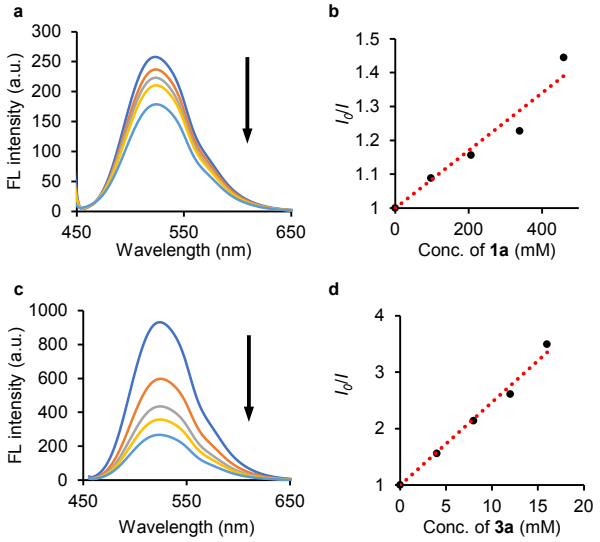

Fig. 4 (a,c) Fluorescence quenching of deprotonated **PS1** (generated in situ from **PS1** and Cs_2CO_3) in the presence of (a) **1a** and (c) **3a**. (b,d) The ratios of fluorescence intensities at 524 nm (I_0/I) in the presence (I) and absence (I_0) of the quenchers (b) **1a** and (d) **3a** as functions of the quencher concentrations. Solvent: DMSO, concentration of **PS1**: 20 μM, concentration of Cs_2CO_3: saturated, excitation wavelength: 440 nm.

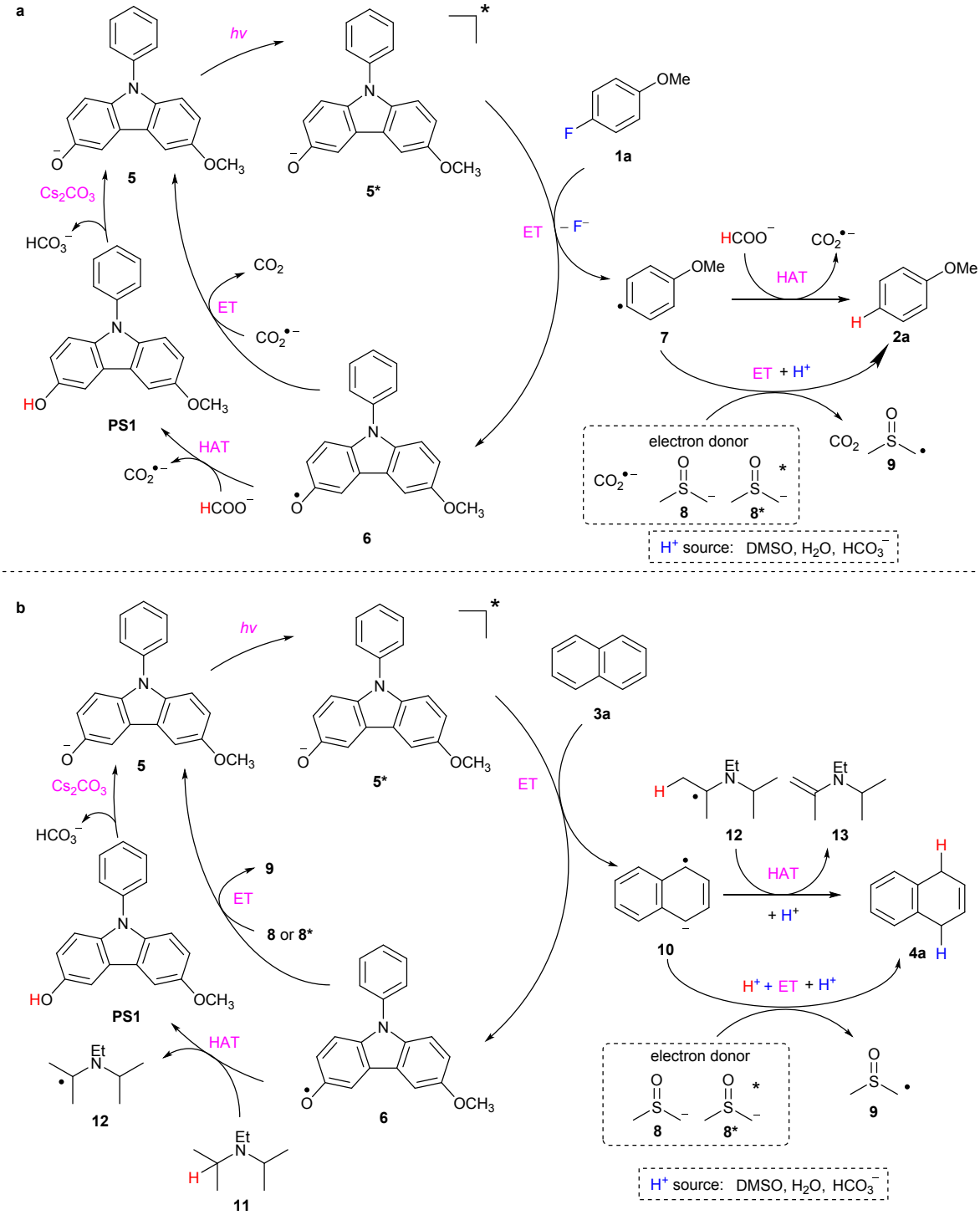

Fig. 5 Proposed reaction mechanisms for photochemical (a) hydrodefluorination and (b) Birch-type reduction. Compounds **1a** and **3a** are shown as the representative substrates in each reaction.

the fluoroarene **1a** (E_{red} = ca. –3.1 V vs SCE),[9, 18, 34-35] followed by the dissociation of fluoride,[6, 9, 18] to afford the aryl radical species **7** along with the carbazolyl oxyl radical **6.** Because the ET process from **5*** to **1a** is slightly uphill in energy, the coordination of a cesium cation to the fluoride atom of **1a** may play a role in enhancing the electron-accepting ability of **1a**.[33] The aryl radical **7** (anisole C(sp^2)–H bond dissociation energy (BDE) > 100 kcal mol^{-1})[36] then undergoes hydrogen atom transfer (HAT) with formate (C(sp^2)–H BDE = 86 kcal mol^{-1})[37] to yield the hydrodefluorinated product **2a** along with a CO_2 radical anion ($CO_2^{\bullet-}$).[37-39] This HAT process was supported by a deuterium labelling experiment using deuterated formate (Section S12). Alternatively, the aryl radical **7**[40-41] can be converted to **2a** through ET and a protonation (PT) process, wherein $CO_2^{\bullet-}$ (E_{ox} = –2.2 V vs SCE)[37], the dimsyl anion **8** (E_{ox} = –0.8 or –0.5 V vs SCE),[42] and/or its excited state **8***[43] are potential

electron donors, and DMSO, water,[32] and/or HCO_3^- are proton donors; the formation of **8** from DMSO and Cs_2CO_3 was experimentally confirmed (See Section S13). The carbazol-3-olate **5** (E_{red} = –0.31 V vs SCE) is regenerated from **6** through ET from $CO_2^{\bullet-}$ generated in the aforementioned HAT process. Alternatively, **6** may be converted to **PS1** via the HAT, for which formate is a potential hydrogen atom donor. While this HAT process is thermodynamically unfavorable (O–H of **PS1** BDE (calculated)[44] = 80.7 kcal mol^{-1}), the subsequent deprotonation of **PS1** may provide the driving force needed to make the overall process feasible. The reaction quantum yield for the hydrodefluorination of **1a** was determined to be 0.91 (Section S15), which implies a chain propagation mechanism may also be operative (Section S16).

The proposed reaction mechanism for Birch-type reduction reaction is shown in Fig. 5b. Naphthalene (**3a**) (E_{red} = –2.71 V vs SCE)[45] undergoes ET with **5*** to form the radical anion **10** and radical **6**. Due to the low reduction potential of **6**, ET from *i*Pr_2NEt to **6** is not plausible. Instead, dimsyl anion **8** and/or its excited state **8*** can serve as electron donors to regenerate **5**. Alternatively, **5** is regenerated through HAT between the amine **11** (C_α–H BDE (calculated)[44] = 90.9 kcal mol^{-1}) and radical **6** to afford **PS1** and radical **12**, followed by deprotonation of the resultant **PS1**. As in the case of hydrodefluorination, the thermodynamic disadvantage of the HAT process may also be compensated by subsequent deprotonation, thereby enabling the reaction to proceed. The radical anion **10** is converted to the product **4a** via either HAT followed by the PT pathway or a sequence of PT, ET, and PT. In these processes, the radical **12** functions as the hydrogen atom donor, while **8** and/or **8*** act as the electron donors, and DMSO, water,[32, 46] and/or HCO_3^- serve as the proton donors.[47] The product formation observed in the absence of PS (11% yield, Table 1, entry 4) is likely attributable to the dimsyl anion, acting as a photo-activated electron donor. The reaction quantum yield for the Birch-type reduction of **3a** was determined to be 0.15 (Section S15), suggesting that the involvement of a chain propagation mechanism need not be considered.

Conclusions

In this study, carbazol-3-olate, generated in situ from carbazol-3-ol via deprotonation, was developed as a novel PS capable of catalyzing challenging photochemical reduction reactions. The carbazol-3-olate PS is distinguished by its transition-metal-free nature, broad visible-light absorption, high reducing ability, and prolonged excited-state lifetime. Using this newly developed PS, both hydrodefluorination and Birch-type reduction reactions were successfully achieved under 480-nm visible light irradiation.[48-49] Ongoing research in our laboratory aims to explore further applications of carbazol-3-olates as PSs, as well as to extend this concept toward the development of new PSs with enhanced properties.

Author contributions

H. K. and R. M. conceived the study. H. K., assisted by W. X., T. Y., M. Hayashi, and R. M., performed most of the experiments. M. F. and Y. K. performed fluorescence lifetime measurements. M. Higashi performed computational studies. N. S. and S. A. performed fluorescence quantum yield measurements. M. Higashi., Y. K., and R. M. analyzed the data and wrote the paper with inputs from all authors. All authors discussed the results and commented on the paper.

Conflicts of interest

There are no conflicts to declare.

Data availability

All data supporting the findings of this study, including details of the experimental study, are available in the article and ESI.

Acknowledgements

This work was supported by JSPS KAKENHI (JP24K01487, JP24K08430, JP23H03961, JP23H00309, JP22H00344, JP20H05835, JP20H05839, and JP20H05831), JST CREST (JPMJCR2316), JST SPRING (JPMJSP2148), and NORITZ Nukumori Foundation (RS2313, RS2407). We thank Ms. Tomoko Amimoto from the Natural Science Center for Basic Research and Development (N-BARD), Hiroshima University for mass analysis measurements [NBARD-00280]. We also thank Prof. Atsunori Mori, Prof. Kentaro Okano, and the students in their laboratory from Kobe University for Karl-Fischer titration.

Notes and references

1 N. A. Romero and D. A. Nicewicz, Organic Photoredox Catalysis, *Chem. Rev.* 2016, **116**, 10075-10166.

2 J. T. Moore, M. J. Dorantes, Z. Pengmei, T. M. Schwartz, J. Schaffner, S. L. Apps, C. A. Gaggioli, U. Das, L. Gagliardi, D. A. Blank and C. C. Lu, Light-Driven Hydrodefluorination of Electron-Rich Aryl Fluorides by an Anionic Rhodium-Gallium Photoredox Catalyst, *Angew. Chem. Int. Ed.* 2022, **61**, e202205575.

3 J. P. Cole, D.-F. Chen, M. Kudisch, R. M. Pearson, C.-H. Lim and G. M. Miyake, Organocatalyzed Birch Reduction Driven by Visible Light, *J. Am. Chem. Soc.* 2020, **142**, 13573-13581.

4 A. Chatterjee and B. König, Birch-Type Photoreduction of Arenes and Heteroarenes by Sensitized Electron Transfer, *Angew. Chem. Int. Ed.* 2019, **58**, 14289-14294.

5 S. M. Senaweera, A. Singh and J. D. Weaver, Photocatalytic Hydrodefluorination: Facile Access to Partially Fluorinated Aromatics, *J. Am. Chem. Soc.* 2014, **136**, 3002-3005.

6 P. Dai, J. Ma, W. Huang, W. Chen, N. Wu, S. Wu, Y. Li, X. Cheng and R. Tan, Photoredox C–F Quaternary Annulation Catalyzed by a Strongly Reducing Iridium Species, *ACS Catal.* 2018, **8**, 802-806.

7 M. Fukui, A. Tanaka and H. Kominami, Photocatalytic Reductive Defluorination of Fluorinated Compounds in Aqueous Alcohol Suspensions of a Metal-loaded Titanium(IV) Oxide, *ChemCatChem* 2020, **12**, 3298-3305.

8 R. Matsubara, T. Yabuta, U. M. Idros, M. Hayashi, F. Ema, Y. Kobori and K. Sakata, UVA- and Visible-Light-Mediated Generation of Carbon Radicals from Organochlorides Using Nonmetal Photocatalyst, *J. Org. Chem.* 2018, **83**, 9381-9390.
9 N. Toriumi, K. Yamashita and N. Iwasawa, Metal-Free Photoredox-Catalyzed Hydrodefluorination of Fluoroarenes Utilizing Amide Solvent as Reductant, *Chem. Eur. J.* 2021, **27**, 12635-12641.
10 J. P. Soumillion, P. Vandereecken and F. C. De Schryver, Photodechlorination of chloroaromatics by electron transfer from an anionic sensitizer, *Tetrahedron Lett.* 1989, **30**, 697-700.
11 G. Filippini, M. Nappi and P. Melchiorre, Photochemical direct perfluoroalkylation of phenols, *Tetrahedron* 2015, **71**, 4535-4542.
12 M. Schmalzbauer, M. Marcon and B. König, Excited State Anions in Organic Transformations, *Angew. Chem. Int. Ed.* 2021, **60**, 6270-6292.
13 G. Filippini, J. Dosso and M. Prato, Phenols as Novel Photocatalytic Platforms for Organic Synthesis, *Helv. Chim. Acta* 2023, **106**, e202300059.
14 E. Hasegawa, T. Tanaka, N. Izumiya, T. Kiuchi, Y. Ooe, H. Iwamoto, S.-y. Takizawa and S. Murata, Protocol for Visible-Light-Promoted Desulfonylation Reactions Utilizing Catalytic Benzimidazolium Aryloxide Betaines and Stoichiometric Hydride Donor Reagents, *J. Org. Chem.* 2020, **85**, 4344-4353.
15 K. Liang, Q. Liu, L. Shen, X. Li, D. Wei, L. Zheng and C. Xia, Intermolecular oxyarylation of olefins with aryl halides and TEMPOH catalyzed by the phenolate anion under visible light, *Chem. Sci.* 2020, **11**, 6996-7002.
16 K. Liang, T. Li, N. Li, Y. Zhang, L. Shen, Z. Ma and C. Xia, Redox-neutral photochemical Heck-type arylation of vinylphenols activated by visible light, *Chem. Sci.* 2020, **11**, 2130-2135.
17 M. Schmalzbauer, T. D. Svejstrup, F. Fricke, P. Brandt, M. J. Johansson, G. Bergonzini and B. König, Redox-Neutral Photocatalytic C–H Carboxylation of Arenes and Styrenes with CO_2, *Chem* 2020, **6**, 2658-2672.
18 S. Wu, F. Schiel and P. Melchiorre, A General Light-Driven Organocatalytic Platform for the Activation of Inert Substrates, *Angew. Chem. Int. Ed.* 2023, **62**, e202306364.
19 C. Liu, N. Shen and R. Shang, Photocatalytic defluoroalkylation and hydrodefluorination of trifluoromethyls using *o*-phosphinophenolate, *Nat. Commun.* 2022, **13**, 354.
20 N. Shen, R. Li, C. Liu, X. Shen, W. Guan and R. Shang, Photocatalytic Cross-Couplings of Aryl Halides Enabled by o-Phosphinophenolate and o-Phosphinothiophenolate, *ACS Catal.* 2022, **12**, 2788-2795.
21 C. Liu, Y. Zhang and R. Shang, BINOLates as potent reducing photocatalysts for inert bond activation and reduction of unsaturated systems, *Chem* 2024, 102359.
22 C. Rosso, S. Cuadros, G. Barison, P. Costa, M. Kurbasic, M. Bonchio, M. Prato, L. Dell'Amico and G. Filippini, Unveiling the Synthetic Potential of Substituted Phenols as Fully Recyclable Organophotoredox Catalysts for the Iodosulfonylation of Olefins, *ACS Catal.* 2022, **12**, 4290-4295.
23 R. Matsubara, T. Shimada, Y. Kobori, T. Yabuta, T. Osakai and M. Hayashi, Photoinduced Charge-Transfer State of 4-Carbazolyl-3-(trifluoromethyl)benzoic Acid: Photophysical Property and Application to Reduction of Carbon-Halogen Bonds as a Sensitizer, *Chem. Asian J.* 2016, **11**, 2006-2010.
24 R. Matsubara, Y.-S. Shin, T. Shimada and M. Hayashi, Revisiting the Saito Photochemical Reduction and the Development of a One-Pot Deoxygenation of Alcohols, *Asian J. Org. Chem.* 2014, **3**, 1054-1057.
25 S. M. Bonesi, M. Mesaros, F. M. Cabrerizo, M. A. Ponce, G. M. Bilmes and R. Erra-Balsells, The photophysics of nitrocarbazoles used as UV-MALDI matrices: Comparative spectroscopic and optoacoustic studies of mononitro- and dinitrocarbazoles, *Chem. Phys. Lett.* 2007, **446**, 49-55.
26 B. Shen, M. W. Bedore, A. Sniady and T. F. Jamison, Continuous flow photocatalysis enhanced using an aluminum mirror: rapid and selective synthesis of 2'-deoxy and 2',3'-dideoxynucleosides, *Chem. Commun.* 2012, **48**, 7444-7446.
27 T. Yabuta, M. Hayashi and R. Matsubara, Photocatalytic Reductive C–O Bond Cleavage of Alkyl Aryl Ethers by Using Carbazole Catalysts with Cesium Carbonate, *J. Org. Chem.* 2021, **86**, 2545-2555.
28 W. Xie, J. Xu, U. Md Idros, J. Katsuhira, M. Fuki, M. Hayashi, M. Yamanaka, Y. Kobori and R. Matsubara, Metal-free reduction of CO_2 to formate using a photochemical organohydride-catalyst recycling strategy, *Nat. Chem.* 2023, **15**, 794-802.
29 R. Matsubara, H. Kuang, T. Yabuta, W. Xie, M. Hayashi and E. Sakuda, Photophysical and electrochemical properties of 9-naphthyl-3,6-diaminocarbazole derivatives and their application as photosensitizers, *J. Photochem. Photobiol.* 2023, **15**, 100176.
30 N. Shen, C. Liu, X. Zhang and R. Shang, o-Phosphinodiarylamides as Reductive Photocatalysts for Dehalogenative and Deaminative Cross-Couplings, *ACS Catal.* 2023, **13**, 11753-11761.
31 M. Chen, Y. Cui, X. Chen, R. Shang and X. Zhang, C–F bond activation enables synthesis of aryl difluoromethyl bicyclopentanes as benzophenone-type bioisosteres, *Nat. Commun.* 2024, **15**, 419.
32 The DMSO used in this study contains 800 ppm w/w of water, as determined by the Karl-Fischer method. This corresponds to 0.5 equivalents of water relative to the substrate in the reaction. A. Johnson and A. Jones, Testing for Water in DMSO: Exploring Alternatives to Volumetric Karl Fischer Analysis, *Pharmaceutical Technology* 2019, **43**, 44-48.
33 Despite the higher oxidation potential of the employed PSs in its excited state than the reduction potential of **1a**, ET proceeded. This is likely due to the interaction between the cesium cation and the fluorine atom of **1a**, which enhances its electron-accepting ability. This hypothesis is consistent with the drastic decrease in yield upon replacing Cs_2CO_3 with K_2CO_3 (entry 12, Table S2).
34 F. Glaser, C. B. Larsen, C. Kerzig and O. S. Wenger, Aryl dechlorination and defluorination with an organic super-photoreductant, *Photochem. Photobiol. Sci.* 2020, **19**, 1035-1041.
35 Estimated value from the reduction potentials of PhCl (-2.78 V vs SCE), *p*-$MeOC_6H_4Cl$ (-2.9 V vs SCE), and PhF (-2.97 V vs SCE). See ref. 9, 18, and 34.
36 S. J. Blanksby and G. B. Ellison, Bond Dissociation Energies of Organic Molecules, *Acc. Chem. Res.* 2003, **36**, 255-263.
37 S. N. Alektiar, J. Han, Y. Dang, C. Z. Rubel and Z. K. Wickens, Radical Hydrocarboxylation of Unactivated Alkenes via Photocatalytic Formate Activation, *J. Am. Chem. Soc.* 2023, **145**, 10991-10997.
38 J. Majhi and G. A. Molander, Recent Discovery, Development, and Synthetic Applications of Formic Acid Salts in Photochemistry, *Angew. Chem. Int. Ed.* 2024, **63**, e202311853.
39 W. Xiao, J. Zhang and J. Wu, Recent Advances in Reactions Involving Carbon Dioxide Radical Anion, *ACS Catal.* 2023, **13**, 15991-16011.

40 The reduction potential of **7** is estimated to be around 0 V vs SCE, based on that of phenyl radical (+0.05 V vs SCE).

41 A. F. Chmiel, O. P. Williams, C. P. Chernowsky, C. S. Yeung and Z. K. Wickens, Non-innocent Radical Ion Intermediates in Photoredox Catalysis: Parallel Reduction Modes Enable Coupling of Diverse Aryl Chlorides, *J. Am. Chem. Soc.* 2021, **143**, 10882-10889.

42 H. Lund, H. Svith, S. U. Pedersen and K. Daasbjerg, Versatile electrochemically based preparation of unusual Grignard reagents containing electrophilic substituents, *Electrochim. Acta* 2005, **51**, 655-664.

43 Y. Huang, Q. Zhang, L.-L. Hua, L.-W. Zhan, J. Hou and B.-D. Li, A versatile catalyst-free redox system mediated by carbon dioxide radical and dimsyl anions, *Cell Rep. Phys. Sci.* 2022, **3**, 100994.

44 For calculations of BDEs, see Section S14.

45 A. Karagiannis, H. Neugebauer, R. A. Lalancette, S. Grimme, A. Hansen and D. E. Prokopchuk, Pushing the Limits of Organometallic Redox Chemistry with an Isolable Mn(−I) Dianion, *J. Am. Chem. Soc.* 2024, **146**, 19279-19285.

46 When dry DMSO (16 ppm w/w of water content) was used, the product yield slightly decreased. This result does not contradict the notion that water serves as a proton donor and affects the reaction kinetics. See Section S17 for detail.

47 The possibility that radical anion **10** undergoes further ET to form a naphthalene dianion, followed by two successive PTs, cannot be ruled out given the stability of the naphthalene dianion. J. Smid, A Stable Dianion of Naphthalene, *J. Am. Chem. Soc.* 1965, **87**, 655-656.

48 During the preparation of this manuscript, studies reporting transition metal-free PS-catalyzed C-F bond activation were published. H. Zhang, J.-X. Chen, J.-P. Qu and Y.-B. Kang, Photocatalytic low-temperature defluorination of PFASs, *Nature* 2024, **635**, 610-617.

49 X. Liu, A. Sau, A. R. Green, M. V. Popescu, N. F. Pompetti, Y. Li, Y. Zhao, R. S. Paton, N. H. Damrauer and G. M. Miyake, Photocatalytic C-F bond activation in small molecules and polyfluoroalkyl substances, *Nature* 2025, **637**, 601-607.

Data availability statements

Carbazol-3-olate photosensitizers enable photocatalytic hydrodefluorination and Birch-type reduction reactions

Huilong Kuang,[a] Weibin Xie,*[a] Tatsushi Yabuta,[a] Masaaki Fuki,[ab] Masahiro Higashi,[c] Yasuhiro Kobori,*[ab] Nozomi Sakai,[a] Seiji Akimoto,[ab] Masahiko Hayashi,[a] Ryosuke Matsubara*[a]

[a] *Department of Chemistry, Graduate School of Science, Kobe University, 1-1 Rokkodai-cho, Nada-ku, Kobe 657-8501, Japan. E-mail: weibinxie@people.kobe-u.ac.jp, ykobori@kitty.kobe-u.ac.jp, matsubara.ryosuke@people.kobe-u.ac.jp.*

[b] *Molecular Photoscience Research Center, Kobe University, 1–1 Rokkodai–cho, Nada–ku, Kobe 657–8501, Japan.*

[c] *Department of Complex Systems Science, Graduate School of Informatics, Nagoya University, Nagoya, 464-8601, Japan.*

All data supporting the findings of this study, including details of the experimental study, are available in the article and ESI.